SAND2009-0358C

Surface Characterization of High Aspect Ratio Suspended Thin Films in a Large Aperture MOEMS Fabry-Perot Tunable Infrared Filter

Jeremy A. Palmer, *Member, IEEE*, Wen-Ting Hsieh, *Member, IEEE*, Manuel Quijada, Brent Mott, and Matthew A. Greenhouse

***Abstract*— A miniature Fabry-Perot tunable infrared filter under development at the NASA Goddard Space Flight Center is fabricated using micro opto electromechanical systems (MOEMS) technology. Intended for wide-field astrophysical studies in space flight, it features a unique 11-mm diameter aperture structure that consists of a set of opposing suspended thin films 500 nm in thickness, supported by annular silicon disks. Achieving the desired effective finesse in the MOEMS instrument requires minimizing the RMS waviness in the film. This paper presents surface characterization data for the suspended aperture film prior to, and following application of a multi-layer dielectric mirror. A minimum RMS waviness of 38 nm was measured prior to coating. Results show evidence of initial deformation of the silicon support structure due to internal stress in the substrate and thin film layers. Film stress gradients in the dielectric coating on either side of the aperture add convexity and other localized deflections. Optical characterization of the prototype has yielded an effective finesse of 3.8.**

***Index Terms*—tunable filter, Fabry-Perot interferometer, etalon, MOEMS, surface characterization, finesse, suspended thin film**

Manuscript received October ##, 2003. This work was supported in part by the U.S. National Aeronautics and Space Administration Goddard Space Flight Center Infrared Astrophysics Branch. Additional funding was provided by the National Research Council Associateship Programs.

J. A. Palmer was a National Research Council Resident Research Associate at the NASA Goddard Space Flight Center, Infrared Astrophysics Branch, Code 685, Greenbelt, MD 20771 USA. He is now with Sandia National Laboratories, P.O. Box 5800, M.S. 0958 Albuquerque, NM 87158-0958 USA (505-284-9623; fax: 505-844-2894; e-mail: japalme@sandia.gov).

W. T. Hsieh is with Raytheon Corporation, NASA Goddard Space Flight Center, Code 553, Greenbelt, MD 20771 USA, (e-mail: whsieh@pop500.gsfc.nasa.gov).

M. Quijada is with Swales Aerospace Corporation, NASA Goddard Space Flight Center, Code 543, Greenbelt, MD 20771 USA, (e-mail: mquijada@pop500.gsfc.nasa.gov).

D. B. Mott is with the NASA Goddard Space Flight Center Detector Systems Branch, Code 553, Greenbelt, MD 20771 USA (e-mail: Brent.Mott@nasa.gov).

M. A. Greenhouse is with the NASA Goddard Space Flight Center Infrared Astrophysics Branch, Code 685, Greenbelt, MD 20771 USA (e-mail: Matt.Greenhouse@ nasa.gov).

I. Introduction

NASA's Origins program seeks to address humanity's most fundamental questions concerning the existence and uniqueness of life in our universe. A new approach to this age-old conundrum is to exploit recent advances in visible/near infrared coronagraphic imagery that facilitate detection of distant extra-solar planets using space-based, wide field optical sensors. One example is the Fabry-Perot (FP) tunable infrared filter, also referred to as a Fabry-Perot interferometer, or tunable etalon (Hecht), [1]). A compact FP tunable infrared filter based on micro opto electromechanical systems (MOEMS) technology has been developed at the NASA Goddard Space Flight Center (GSFC) to sense corona emissions in the 1.1 to 2.3 um band. It is designed with a novel 11-mm diameter aperture for imaging spectrograph applications in 8-m class space telescopes, and similar astronomical instruments. Prior to this point, MOEMS FP tunable filters with aperture dimensions not exceeding 4 mm have been demonstrated (Raley, Ciarlo, Koo, Beiriger, Trujillo, Yu, Loomis, and Chow; Tran, Lo, Zhu, Haronian, and Mozdy; Jerman, Clift, and Mallinson; Bartek, Correia, and Wolffenbuttel) [2, 3, 4, 5, 6]. As a later section explains, the optical performance of the tunable infrared filter is influenced by the waviness of high aspect ratio (on the order of 10^4) suspended thin films that form the aperture structure. This paper describes a series of surface characterization trials that measured aperture waviness before and after multilayer dielectric mirrors were applied. An analysis was performed that calculates the effective finesse of the tunable infrared filter based on waviness measurements of the coated prototype, and estimates of parallelism deviation of the optical surfaces. Finesse was then measured directly and compared to (1) the result of the analysis and, (2) the desired value. The analysis leads to significant observations regarding the capability and limitations of the large aperture MOEMS FP instrument that incorporates a coated, high aspect ratio suspended thin film.

The architecture of a conventional Fabry-Perottunable etalon is similar to that of the modern laser cavity [1]. It consists of two parallel glass plates separated by a gap (d) as indicated in Figure 1. The gap-facing surfaces are polished flat and coated such that their reflectance is slightly less than 100% (Barry, Satyapal, Greenhouse, Barclay, Amato, Arritt,

Brown, Harvey, Holt, Kuhn, Lesyna, Fonneland, and Hilgeman), [8]. A fraction of incoming light from a broad-band, diffuse, and collimated source enters the gap, and

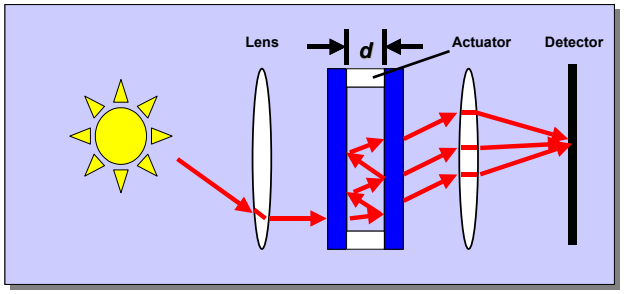

Fig. 1. Conventional Fabry-Perot instrument.

multiple reflections occur as shown [1]. Specific wavelengths λ are resonant according to the magnitude of the gap *d*. If the phase changes associated with the multiple reflections within the gap are neglected, this relationship is defined by the following expression (Atherton, Reay, and Ring), [12]:

$$m\lambda = 2nd\cos\theta \quad (1)$$

where *m* is the order of interference, *n* is the refractive index of the medium between the plates (in this application, *n = 1.00* for air or vacuum), and θ is the angle of incident rays on the instrument. In this study, normal incidence is assumed. At resonance, the reflected rays within the gap interfere destructively, and the light passes through the instrument to a detector [12]. Adjusting the magnitude of the gap alters the resonant wavelength. In the past, controlled tuning was provided by piezoelectric translators coupled with capacitive feedback sensors. In space flight applications, the bulk, precision engineering, and delicate nature of the conventional FP instrument make it susceptible to damage, especially during the launch phase [8]. Furthermore, piezoceramic performance degrades in the (30 K) cryogenic environment of space [8]. Effectively utilizing a compact, electrostatically driven MOEMS design (one with low thermal mass for rapid cooling, and high natural frequency) mitigates these risks.

The GSFC MOEMS FP tunable infrared filter shown in Figure 2 consists of an upper movable plate, and a fixed lower plate. They are constructed from 330-um thick silicon wafers

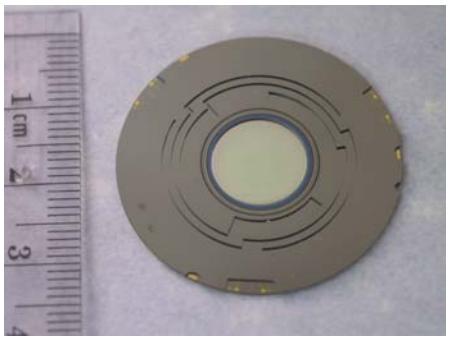

Fig. 2. GSFC MOEMS Fabry-Perot tunable infrared filter prototype.

(100 orientation), coated with a 400-nm layer of silicon dioxide, and an overlying layer of 500-nm thick silicon nitride (see Figure 3). Up to four upper or lower plates are microfabricated on a single 4-inch wafer using similar processes. The following is a description of the process for the upper plate, illustrated in Figure 3. In the initial steps, the aperture area in the center of the instrument is defined in addition to insulating dielectric layers for electrical conductors. This is accomplished by patterning and etching the nitride and oxide layers using lithography, and a combination of Reactive Ion Etching (RIE) and buffered hydroflouric acid to remove the oxide. Next, layers of gold and titanium are evaporated onto the substrate, and subsequently patterned and etched, to complete the network of actuation/sense patches, electrical leads, and wire terminals shown in Figure 4. An Electron Cyclotron Resonance ECR

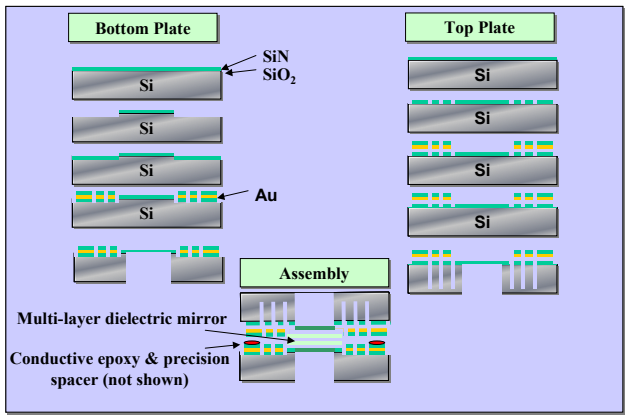

Fig. 3. Microfabrication process.

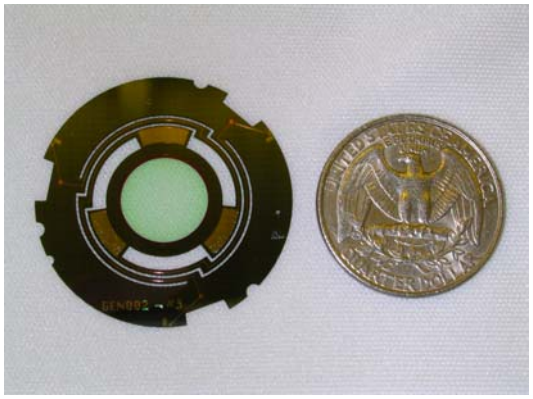

Fig. 4. FP upper plate (gap-facing side)showing actuation/sense network.

apparatus is used to deposit a 700-nm silicon dioxide passivation layer on the gold traces. The aperture surface and movable support structure of the upper plate are bulk micromachined using Deep Reactive Ion Etching (DRIE) technology. Preparation for DRIE includes bonding a pyrex backing wafer to the substrate, and patterning a thick layer of photoresist on the opposite (non-gap facing) side. DRIE removes bulk silicon from the aperture area, leaving the

suspended oxide and nitride films in a state of drum-like tension (the oxide film is ultimately removed, and the suspended nitride remains). Concurrently, the bulk micromachining defines a set of narrow flexures that join the aperture structure to the perimeter of the upper plate (see Figure 4). A dielectric mirror, consisting of alternating layers of niobium pentoxide and silicon dioxide, is deposited on each side of the aperture film. In the final steps of the fabrication process, the tunable infrared filter is assembled by the mating the coated upper and lower plates as shown in Figure 4. The plates are electrically connected with silver-filled epoxy applied to opposing terminals. Twenty-five mirometer diameter gold wire is inserted between the plates that sets the distance between the actuation/sense patches at 18 to 20 um. The nominal optical gap (d) of the assembled device with five-layer dielectic mirrors is approximately 18 um. Applying a potential between the actuation/sense patches generates an electric field, and a corresponding attractive force, that causes the suspended upper optical area to deflect downward toward the lower, hence altering the magnitude of the gap. Complete details of MOEMS FP actuation are provided by Kuhn *et al.* (Kuhn, Barclay, Greenhouse, Mott, and Satyapal), [10].

II. Analysis

Table 1 lists the microfabrication and optical performance objectives of the large aperture MOEMS FP tunable infrared filter program. Objectives for parallelism

TABLE I
MOEMS FP PROGRAM PERFORMANCE OBJECTIVES

Parameter	Symbol [12]	Objective
Effective finesse	N_E	50
Aperture waviness	δt_w	6 nm root-mean-square (RMS)
Parallelism	δt_p	10 nm

and aperture waviness were established from experience with conventional space-based FP systems, such as the Demonstration Unit for Low-order Cryogenic Etalon (DULCE), [8]. Referring to Table 1, the aperture waviness objective of 6 nm represents approximately one hundredth of the emission wavelength of the helium-neon laser used in optical characterizations of DULCE. As the following segment explains, the effective finesse depends upon these parameters.

Finesse is a primary measure of performance in the FP instrument, and is analagous to the quality factor Q of an oscillator (Guenther), [13]. Finesse in the ideal FP system is independent of the magnitude of the gap, and is defined as the ratio of the wavelength range between resonant peaks of adjacent order (referred to as the *free spectral range*), and the full width half maximum (FWHM) of a given peak [12,13]. In reality, the effective finesse, N_{eff}, defines performance [12]. Effective finesse accounts for increases in the FWHM due to diffraction in the aperture, surface roughness, reflectance, flatness, and parallelism of the plates [12,13]. Effective finesse of the FP prototype was measured directly using a Bruker™ radiometer with a collimated broad band source. Since the beam diameter was less than that of the prototype aperture, the contribution to the effective finesse due to diffractive effects was not considered in the analysis. Furthermore, scanning electron microscope (SEM) observations of the aperture surface suggested roughness values on the order of angstroms. Consequently, the contribution due to surface roughness was also omitted.

The component of the effective finesse associated with the reflectance of the mirror surfaces is expressed as the following [12]:

$$N_R = \frac{\pi\sqrt{R}}{(1-R)} \tag{2}$$

where R is the reflectance of the mirror at normal incidence measured with a similar Perkin Elmer™ radiometer. Defects in parallelism (δt_p) of the plates are considered in the following expression for the parallelism finesse [12]:

$$N_p = \frac{\lambda}{\sqrt{3}\delta t_p}. \tag{3}$$

In trials with the prototype FP filter, direct interferometric measurements of parallelism deviations were not performed. Alternatively, the effective finesse calculation is run for varying estimates of the deviation based on a series of observations of the prototype with a confocal microscope. Waviness in either the upper or lower mirror surfaces (δt_w) is captured by the figure finesse [12,13]:

$$N_f = \frac{\lambda}{2\delta t_w}. \tag{4}$$

The root-mean-square (RMS) waviness as a fraction of the wavelength λ used in (4) was measured with a Zygo™ interferometer with a 546 nm source. Finally, the effective finesse N_E of the FP tunable infrared filter is expressed as [12,13]:

$$N_E = \frac{1}{\sqrt{\frac{1}{N_R^2}+\frac{1}{N_P^2}+\frac{1}{N_f^2}}}. \tag{5}$$

III. Results

Seventeen MOEMS FP prototype plates (eight upper plates, and nine lower plates) were fabricated and mounted in protective fixtures. The gap-facing side of the uncoated aperture film was characterized using the Zygo™ interferometer, yielding a map of the aperture surface, and a measurement of the RMS waviness. Two sets of plates exhibiting the lowest measured RMS waviness were selected, and multi-layer dielectric mirror coatings were subsequently applied. Waviness measurements were repeated on the coated samples.

The uncoated samples displayed two distinct surface contours. Uncoated lower plate aperture films exhibited the so-called *complex saddle* contour as described by Jacobson *et al.* (Jacobson, Barclay, Greenhouse, Mott, Satyapal, and King; [9], see Figure 5, below). Upper plate aperture films

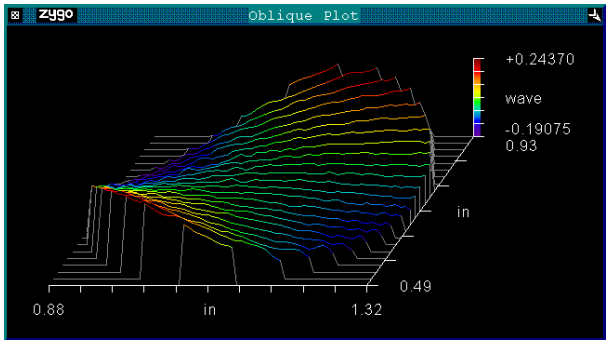

Fig. 5. Uncoated lower plate aperture film surface map showing complex saddle contour [9].

showed both the complex saddle, *and* the six-pointed star contour shown in Figure 6 [9]. RMS waviness

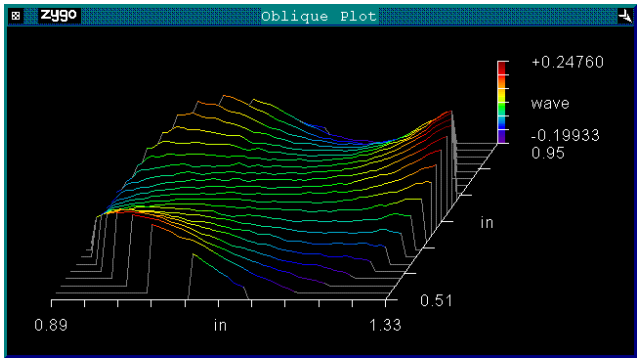

Fig. 6. Uncoated upper plate aperture film surface map showing six-pointed star contour [9].

measurements for the aperture films of the uncoated lower plates ranged from a maximum of 248 nm to a minimum of 42 nm, while the uncoated upper plate films ranged from 187 nm to 38 nm. Examinations of the upper and lower plate data sets suggest significant variance in RMS waviness among devices that were fabricated on the same wafer. This observation was consistent for the majority of wafers in the characterization. The RMS waviness of the aperture films increased after the multi-layer dielectric mirror coating was applied. The minimum RMS waviness in the two upper plate samples increased from 38 nm to 70 nm (84%), whereas the minimum of the lower plate samples increased from 42 nm to 60 nm (43%) after coating. Figure 7 depicts the coated aperture film contour for a lower plate. A supplementary

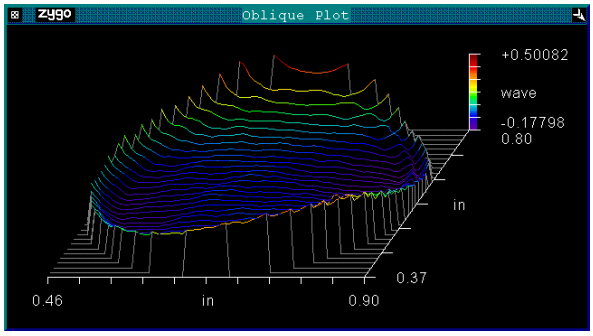

Fig. 7. Lower plate aperture film surface map following multi-layer dielectric mirror coating.

study focused on surface mapping of the silicon support structure surrounding the aperture. These results, combined with a review of prior work [9] and coating process measurements, offered important insight into the trends in aperture film waviness. First, the silicon structure surrounding the aperture film was observed to have a similar surface contour. More importantly, the deflected profile was largely unchanged after all films were removed from the substrate. This condition suggests that flatness deviations in the aperture film are not exclusively a consequence of thin film stresses, but also residual stress in the substrate. The fact that the unprocessed wafers exhibited measurable "bow," or curvature, supports this premise. Secondly, witness sample measurements revealed a stress gradient of 3 MPa in the multi-layer dielectric mirror coatings on each side of the aperture film. The gradient may contribute to the apparent increase in waviness after coating.

The aforementioned coated plates were assembled to construct two MOEMS FP tunable infrared filter prototypes. Prior to assembly, the reflectance of the individual coated aperture surfaces was measured. Reflectance data, together with RMS waviness measurements, are reported in Table 2. The rightmost column lists the corresponding contribution to the effective finesse as calculated by (2), and (4). The final effective finesse predictions are shown in Table 3 for estimates of the plate parallelism deviation varying over three orders of magnitude. Predictions vary according to which data set is used in the calculation: that of the upper aperture surface, or the lower. In this study, the effective finesse resulting from an estimated parallelism deviation of one micrometer or greater is considered the most realistic.

TABLE II
ANALYSIS DATA FOR COATED PROTOTYPE[1]

Parameter	Upper Aperture Surface	Lower Aperture Surface	Component of Effective Finesse Upper, (Lower)
Maximum reflectance (%)	92.8	91.6	42, (36)
RMS waviness (nm)	70	152	15, (7)

[1]All measurements correspond to a wavelength of 2.1 micrometers.

TABLE III
EFFECTIVE FINESSE RESULTS

Result	Plate Parallelism Deviation (nm)		
	1000	100	10
Analysis using upper aperture surface data	1.2	9.2	14
Analysis using lower aperture surface data	1.2	5.9	6.8
Direct measurement	3.8		

However, the results stemming from lower estimates are included to illustrate the positive performance impact of minimizing the parallelism deviation. In practice, this is accomplished by closed-loop control of the electrostatic actuation mechanism using the system's capacitive position sensing capability. The effective finesse of the prototype was directly measured from the plot of transmittance versus wavelength shown in Figure 8. Note that due to errors in the

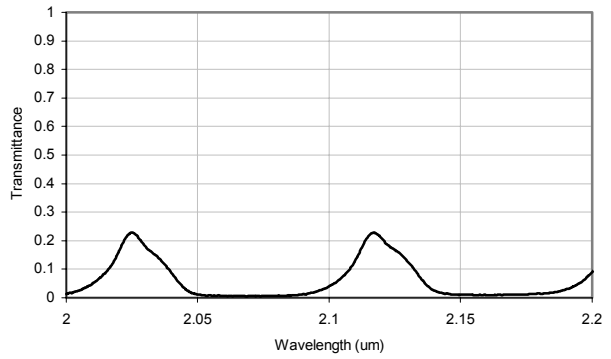

Fig. 8. Transmittance versus wavelength for the MOEMS FP prototype.

placement of the spacer material during prototype assembly, the coated optical gap is larger than the design. This condition tends to bias the resonance of a given order towards longer wavelengths according to (1). The graphical measurementtechnique yielded a free spectral range of 0.092 micrometers, and a full width half maximum of 0.024 micrometers. It follows that the measured effective finesse of the prototype was 3.8 (see Table 3). Although greater than the analytical prediction, this measurement fell short of the program objective of 50. A simple (albeit expensive) improvement is to boost the aperture reflectivity by applying a more sophisticated multilayer dielectric mirror. However, the analysis suggests that reflectivities as high as 99% have a minor impact. Dramatic enhancements are possible by reducing deviations in waviness and parallelism.

IV. CONCLUSION

The MOEMS FP tunable infrared filter developed at the NASA Goddard Space Center is the first known application of a MOEMS Fabry-Perot instrument in space flight, with aperture width exceeding 10 mm. Surface characterization of the suspended aperture surfaces led to predictions of the effective finesse that were compared to direct measurements of the prototype. The results of the investigation lead to the following conclusions:

- The aperture films exhibit periodic flatness deviations, greater than 40 nm RMS, that increase in amplitude when a multilayer dielectric mirror is applied. The waviness, in conjunction with defects in reflectivity and parallelism, limit the effective finesse of the prototype to a value of 4 or less.
- A strategy for reducing aperture waviness must include not only minimizing stress and stress gradients in the applied coatings, but also flatness defects in the silicon substrate.

Future work on the MOEMS FP tunable infrared filter includes work in two areas: fabrication and control. Fabrication process development focuses on increasing device yields by eliminating photoresist defects and wafer bond voids that destroy the aperture films. Lastly, a feedback control system based integrated capacitive position sensors is necessary to enhance the parallelism of the upper and lower plates.

ACKNOWLEDGMENT

J.A. Palmer would like to thank the staff of the Detector Development Laboratory at the NASA Goddard Space Flight Center for their guidance and support in area of fabrication. Additional thanks go to Mr. Tom French and Joseph McMann of the Mantech Optical Support Function for their service in surface characterization. Lastly, the authors acknowledge Barr Associates, Inc., Westford, MA for the optical coating products used in the study.

REFERENCES

[1] E. Hecht, *Optics*, 2nd ed., San Francisco: Addison Wesley, 2002, pp. 421-423.

[2] T. T. D. Tran, Y. H. Lo, Z. H. Zhu, D. Haronian, and E. Mozdy, "Surface micromachined Fabry-Perot tunable filter," *IEEE Photonics Tcchnology Letters,* vol. 8, no. 3, pp. 393-395, 1996.

[3] N. F. Raley, D. R. Ciarlo, J. C. Koo, B. Beiriger, J. Trujillo, C. Yu, G. Loomis, and R. Chow, "A Fabry-Perot microinterferometer for visible wavelengths," in *Proc. 1992 Solid-State Sensor and Actuator Workshop*, Hilton Head, South Carolina, 1992, pp. 170-173.

[4] J. H. Jerman, D. J. Clift, and S. R. Mallinson, "A miniature Fabry-Perot interferometer with a corrugated silicon diaphragm support," *Sensors and Actuators*, vol. A29, no. 2, pp. 151-158, 1991.

[5] M. Bartek, J. H. Correia, and R. F. Wolffenbuttel, "Micromachined Fabry-Perot optical filters," *Proc. 2nd Int. Conf. Adv. Semicon. Dev. and Microsys.,* Slovakia, 1998, pp. 283 –286.

[6] M. Bartek, J. H. Correia, and R. F. Wolffenbuttel, "Bulk-micromachined tunable Fabry-Perot microinterferometer for the visible spectral range," *Sensors And Actuators,* vol. A76, no. 3, pp. 191-196, 1999.

[7] J. D. Patterson, "Micro-mechanical voltage tunable Fabry-Perot filters formed in (111) silicon," NASA Technical Report 3702, 1997.

[8] R. K. Barry, S. Satyapal, M. A. Greenhouse, R. B. Barclay, D. Amato, B. Arritt, G. Brown, V. Harvey, C. Holt, J. Kuhn, L. Lesyna, N. Fonneland, and T. Hilgeman, "A near IR Fabry-Perot interferometer for wide field, low resolution hyperspectral imaging on the next generation space telescope," NASA Technical Report 20000084158, 2000.

[9] M. B. Jacobson, R. B. Barclay, M. A. Greenhouse, D. B. Mott, S. Satyapal, T. T. King, "Simulation of an electrostatically actuated micro-machined Fabry-Perot etalon," AIAA Paper 2002-5720, 2002.

[10] J. L. Kuhn, R. B. Barclay, M. A. Greenhouse, D. B. Mott, and S. Satyapal, "Electro-mechanical simulation of a large aperture MOEMS Fabry-Perot tunable filter," *Proc. SPIE*, vol. 4178, pp. 325-35, 2000.

[11] D. B. Mott, R. B. Barclay, A. Bier, T. Chen, B. DiCamillo, D. Deming, M. A. Greenhouse, R. Henry, T. Hewagama, M. B. Jacobson, M. Quijada, S. Satyapal, and S. D. Schwinger, "Micro-machined tunable Fabry-Perot filters for infrared astronomy," *Proc. SPIE*, vol. 4841, pp. 578-85, 2003.

[12] P. D. Atherton, N. K. Reay, and J. Ring, "Tunable Fabry-Perot filters," *Optical Engineering*, vol. 20, no. 6, pp. 806-814, 1981.

[13] R. D. Guenther, *Modern Optics*, New York: John Wiley and Sons, 1990, pp. 110-116.

First A. Author (M'76–SM'81–F'87) and the other authors may include biographies at the end of regular papers. Biographies are often not included in conference-related papers. This author became a Member (M) of IEEE in 1976, a Senior Member (SM) in 1981, and a Fellow (F) in 1987. The first paragraph may contain a place and/or date of birth (list place, then date). Next, the author's educational background is listed. The degrees should be listed with type of degree in what field, which institution, city, state or country, and year degree was earned. The author's major field of study should be lower-cased.

The second paragraph uses the pronoun of the person (he or she) and not the author's last name. It lists military and work experience, including summer and fellowship jobs. Job titles are capitalized. The current job must have a location; previous positions may be listed without one. Information concerning previous publications may be included. Try not to list more than three books or published articles. The format for listing publishers of a book within the biography is: title of book (city, state: publisher name, year) similar to a reference. Current and previous research interests ends the paragraph.

The third paragraph begins with the author's title and last name (e.g., Dr. Smith, Prof. Jones, Mr. Kajor, Ms. Hunter). List any memberships in professional societies other than the IEEE. Finally, list any awards and work for IEEE committees and publications. If a photograph is provided, the biography will be indented around it. The photograph is placed at the top left of the biography. Personal hobbies will be deleted from the biography.